Talanta 208 (2020) 120408

Contents lists available at ScienceDirect

Talanta

journal homepage: www.elsevier.com/locate/talanta

Digital image-based quantification of chlorpyrifos in water samples using a lipase embedded paper based device

Karthikumar Sankar[a,*], D. Lenisha[a], G. Janaki[a], J. Juliana[a], R. Shyam Kumar[a], M. Chengathir Selvi[b], G. Srinivasan[b]

[a] Department of Biotechnology, Kamaraj College of Engineering and Technology, S.P.G.C. Nagar, K. Vellakulam, 625 701, Madurai, Tamilnadu, India
[b] Department of Computer Science and Engineering, Kamaraj College of Engineering and Technology, S.P.G.C. Nagar, K. Vellakulam, 625 701, Madurai, Tamilnadu, India

ARTICLE INFO

Keywords:
Lipase
Pesticide
Chlorpyrifos
Paper sensor
Image processing
Smartphone

ABSTRACT

A paper-based device (PBD) for the detection of chlorpyrifos pesticide at field application was fabricated based on the principles of enzyme inhibition and image processing. *Rhizopus niveus* lipase, p-nitrophenol palmitate and Whatman No.1 paper were used as an enzyme, substrate and support matrix, respectively. The performance of functionalized PBD was tested for lateral flow assay reaction in pure water (negative control), artificial pesticide water (positive control) and selected fruits and vegetables wash water (test). The digital image of the PBD after the test was captured using an android smartphone and analyzed in MATLAB software. Different colour space models such as, grey, RGB, HSV and YCbCr were studied and the Cb coordinate was chosen for its higher linearity ($R^2 = 0.988$) with pesticide concentration. Experimental variations such as paper length, relative concentration ratio of the substrate and enzyme were investigated to minimize the product cost and analysis time. The developed PBD showed a significant response over wide range of sample solution's pH and operational temperature. Further, a long-term storage stability was measured for developed PBD. The LOD and LOQ were found to be 0.065 mgL^{-1} and 0.198 mgL^{-1}. The results obtained from newly developed image processing method showed 92.8% accuracy with microtiter plate assay. Higher MRL was determined in the wash water of cauliflower, grapes, coriander leaves, brinjal and bitter guard. Overall, the developed paper biosensor was precise, cost effective and most suitable for field applications.

1. Introduction

Pesticides are widely used in agricultural fields around the globe to increase the crop yield, improve the quality and to protect the food from pest infestation. These pesticide residues enter into the food chain through air, water and soil which cause adverse impacts on human health and environment. It is therefore important to monitor the persistence of these pesticide residues in water and food grown for human consumption. Among many types of pesticides used all over the world, organophosphates (OPs) are synthetic organic pesticides manufactured from carbon chemicals and contain phosphorus integrated by esters of phosphoric, phosphonic, phorothionic or related acids. Many parts of the India are heavily polluted with organophosphate pesticides. More than 80% of the pesticide related hospitalization cases are due to organophosphate pesticide [1]. Chlorpyrifos is one of the OP group of pesticides, which is most commonly used due to its cost-competitive and broad spectrum of activity [2]. In humans, chlorpyrifos poisoning involves competitive inhibition of carboxylic ester hydrolases which results neuronal disorders. It also causes oxidative stress and endocrine disruption [3,4]. Hence, proper monitoring the pesticide residues in human food consumption will prevent the health risk. The conventional analytical methods such as GC-MS and LC-MS techniques are well established for wide range of pesticide detection. However, they are very expensive, laborious and need of trained expertise to execute. Further, these facilities are limited and are not affordable to general public. Owing to health concern, Food Safety and Environmental Protection regulatory authorities demand the researchers to develop rapid, sensitive, user friendly methods to monitor the presence of food, environmental contaminants and toxic substances.

Rising to the challenge, biosensing techniques attract food and environmental analysts in recent years. Many researchers have developed biosensor for the detection of variety of pollutants and hazardous compounds present in the environment [5–7]. Among various biosensing strategies, amperometric biosensors have proven its effectiveness in the qualitative and quantitative analysis of pesticide [8,9]. Recently, Stepenkova [10] and Justino [7] has compiled and presented a detailed

* Corresponding author.
E-mail address: skarthikumar@gmail.com (K. Sankar).

https://doi.org/10.1016/j.talanta.2019.120408
Received 20 June 2019; Received in revised form 27 September 2019; Accepted 28 September 2019
Available online 30 September 2019
0039-9140/

review on various biosensor developed for pesticide detection, in which most of the protocols are colour based assay. A dipstick coated with acetyl choline esterase has been developed for the detection of organophosphate and carbamate pesticides [11]. Recently, Kim [12] has developed colourimetric paper sensor for the detection of pesticides based on the principle of enzyme inhibition. Similarly, the enzyme inhibition concept was applied by Gai [13] in light driven self-powered biosensor to detect organophosphate pesticides which includes chlorpyrifos. Apart from the enzyme biosensor, Kumar [14] developed a whole cell biosensor using *Flavobacterium* sp as the source of organophosphorus hydrolase for the detection of methyl parathion pesticide. Besides, Cho [15] fabricated a dip stick immunosensor for the detection of the organophosphorus insecticide, fenthion. It is coated with a polyclonal antibody raised against parathion-methyl. To develop an efficient biosensor for the detection of pesticides, the assay protocol must be easy and the results must be reliable and rapid. Further, the method of detection should not require the high technical background. One type of biosensor which satisfies these conditions is paper-based sensors which offer a new alternative for fabricating simple, low-cost, portable and disposable analytical device. The major advantages of using paper as a sensing platform include passive liquid transport, compatibility with chemicals/bio-chemicals and fast response. Whatman No. 1 filter paper is widely used solid support by many researchers due to its medium retention and flow rate [16,17]. Inorder to detect the activity of an enzyme, chromogenic substrates are used for the direct visualisation of colour change. In recent years, computer vision system and image processing tools have paved the way for extracting quantitative data sets from visual results of an image by the environmental and food analyst. Image processing technique precisely measures and quantifies the developed colour upon enzyme substrate reaction and eliminates the subjectivity of manual interpretation. This non-destructive method has been used by many researchers in various applications. Wang [18] developed a tree shaped paper strip for the detection of protein concentration and the image of the strip can be used for remote monitoring of food and environmental samples. Similarly, Dungchai [19] fabricated a multiple colourimetric paper-based device which can be used for the detection of glucose, lactate and uric acid. Recently, Thajee [20] has used web camera as a colourimetric sensor for monitoring redox reactions. The organic and inorganic apples were distinguished using image based analysis [21].

Based on the above context, the present work aims to develop a low-cost paper biosensor for rapid determination of chlorpyrifos for point-of-care applications. The paper biosensor is embedded with lipase and p-nitrophenol palmitate (PNPP) as a chromogenic substrate. Enzyme inhibition principle is adopted to detect the chlorpyrifos. The lipase doped in paper sensor is irreversibly inhibited by the chlorpyrifos pesticide present in the sample. The colour change upon the enzyme substrate reaction with and without pesticide is measured using smartphone. Then, the image is processed through custom made image processing algorithm in MATLAB. The concentration of pesticide is determined from the rate of enzyme inhibition. The developed paper biosensor and its protocol demonstrates its simplicity, sensitivity, affordability and portability.

2. Materials and methods

2.1. Enzyme and reagents

Rhizopus niveus Lipase and para-nitrophenyl palmitate (p-NPP) were bought from Sigma-Aldrich, Bangalore and stored at 4 °C. Chlorpyrifos (50%, EC) was purchased from local market, Madurai, Tamilnadu. p-Nitrophenol (p-NP) and Whatmann No. 1 chromatographic paper were purchased from HiMedia, Bangalore. Digital images were captured in a smart phone, Infocus Turbo 5, Model IF9001, android v.70, 13 MP rear camera. Image processing was performed in MATLAB R2015a.

2.2. Pesticide detection in microtiter plate assay method

The lipase assay was performed using p-nitrophenol palmitate as described previously [22]. The yellow colour developed upon the reaction was monitored at $\lambda 410_{nm}$ in microtiter plate reader (BioRAD, Bangalore). The principle of the enzyme reaction is shown in supplementary data (Fig. S1). The lipase activity was calculated from the p-nitrophenol calibration curve. One unit (U) of enzyme activity was defined as the amount of p-nitrophenol released per mg of enzyme in one minute.

Enzyme inhibition principle was adopted to determine the pesticide concentration in aqueous samples. The lipase assay was performed in microtiter plate for the total volume of 250 µL in the presence of chlorpyrifos at 0.2 mgL^{-1} to 1.0 mgL^{-1} concentration. The reaction mixture was kept for 15 min at 37 °C. A reaction without chlorpyrifos was considered as control. The percentage of enzyme inhibition was determined and a calibration curve was constructed by plotting the chlorpyrifos concentration against percentage inhibition.

2.3. Pesticide detection in image processing method

To construct the calibration curve for p-nitrophenol using image processing technique, the digital image of the 96 well plate loaded with different concentration of p-nitrophenol was taken in smart phone camera and subjected to image processing technique in MATLAB R2015a. The flow diagram of the image processing algorithm constructed for the detection of chlorpyrifos is provided in supplementary material (Fig. S2). The mean intensity of the each well in microtiter plate was selected using circle detection algorithm (Fig. S3) and plotted against p-nitrophenol to construct calibration curve. Similarly, the same concentration of p-nitrophenol was applied on paper strip and the images of the papers were subjected to image processing (Fig. S4).

2.3.1. Fabrication of paper-based device

Fig. 1 depicts the dimension of paper sensor and work flow. Initially, paper biosensor was prepared in three dimensions to understand the effect of diffusion limitations. The Whatmann No.1 chromatographic paper was cut into pieces of (A): 1.5 × 12.5 cm, (B): 1.5 × 10 cm and (C): 1.5 × 7.5 cm. A thin paraffin wax coating was applied for about 0.25 cm width at three edges of the paper except the bottom side. The wax coated paper was heated on hot plate for 2 min at 50 °C. The heating process seals the pores and helps in achieving narrow dispersion and uniform flow pattern of the analyte [23]. 5 µL of p-NPP (5 mg mL^{-1}) and 10 µL of lipase (1.0 mg mL^{-1}) were loaded in substrate and enzyme zones, respectively. Bottom edge of the paper left free from wax coating, which enables the sample to flow through the paper by capillary action. The substrate zone was considered as reacting zone or region of interest (ROI). The area between ROI and enzyme zone was considered as background to nullify the effect of interference.

2.3.2. Functionalization of paper-based device

The paper-*based device* detects lipase inhibitor (chlorpyrifos) based on enzyme-substrate reaction. Lipase hydrolyses the colourless p-NPP into yellow coloured p-NP and palmitic acid. As depicted in Fig. 1 the functional paper PBD is immersed in a beaker containing distilled water (negative control), pesticide solution (positive control) and grape fruit wash water (test), separately. Being hydrophilic, the bound enzyme moves along with water towards reacting zone through capillary action. When the sample reaches the stop line, the strip was removed and kept for incubation at 37 °C for 15 min. In the case of negative control, the enzyme reaches the reaction zone without any inhibition and develops a strong yellow colour. If the solution contains pesticide, which inhibits the enzyme before it reaches the reaction zone and causes low or nil yellow colour development. Hence, the pesticide concentration is determined from the percentage of enzyme inhibition.

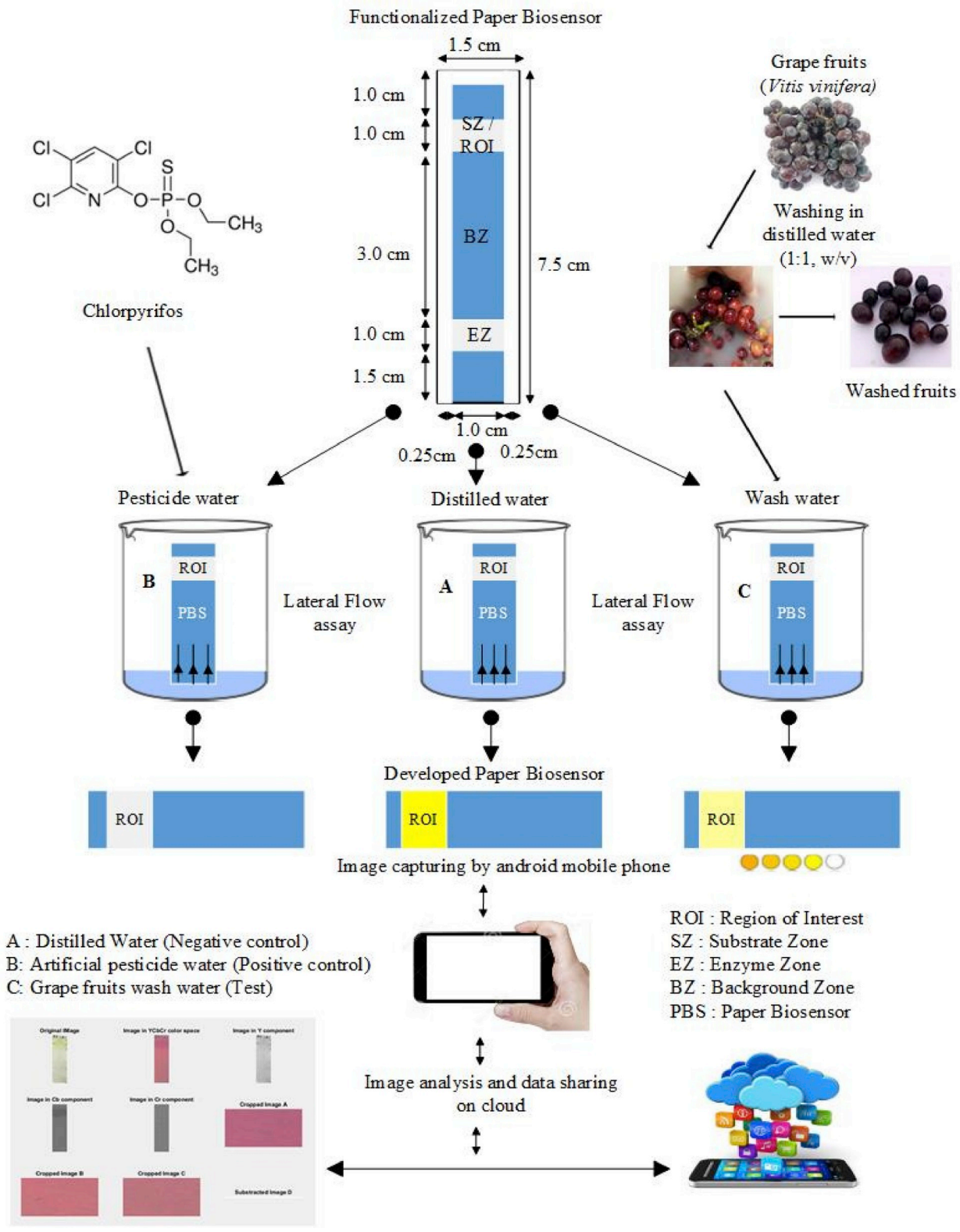

Fig. 1. Illustration of the experimental work flow for the detection of chlorpyrifos in water samples using functionalized paper-based device.

2.3.3. Image capture

The image of the paper sensor after the reaction was captured on a white background using a smartphone. Initially, two sets of lighting systems were used for capturing the images. One is open environment with sufficient illumination and another one is in closed wooden chamber (30 cm × 30 cm x 60 cm) with 22 W LED white light at the bottom and a hole at top to capture the image.

2.3.4. Image analysis

Quantitative analysis of the image of paper sensor was performed in

MATLAB software. An algorithm to measure the percentage of enzyme inhibition was developed. As shown in Fig. S2 the algorithm starts with pre-processing of original RGB input images by applying noise filters. Preprocessed RGB images were converted into other colour space models such as grey, HSV and YCbCr. Then, region of interest (ROI) and background zone were selected and cropped into separate images. The mean intensity value of the background zone was subtracted from mean intensity value of ROI to determine the change in colour. Inorder to determine the colour coordinate that provides best linear fit with p-nitrophenol concentration, each colour component (R - red, G - green, B - blue, H - hue, S – saturation, V – value, Y - luminance, Cb – blue difference and Cr – red difference) were extracted. Then, a calibration curve was constructed by plotting the corrected mean intensity value of ROI against p-nitrophenol concentration. Among various colour component, Cb value showed a linearity with R^2 of 0.98. Hence, the p-nitrophenol concentration on paper strip was determined by interpolating Cb calibration curve. Another calibration curve using mean Cb intensity of RoI and concentration of chlorpyrifos was constructed.

2.4. Determination of enzyme kinetic parameters

Prior to the fabrication of PBD and monitoring the enzyme activity on paper, free enzyme kinetic parameters were determined as mentioned in our previous report [22]. The k_m value was determined from the enzyme reactions with different concentration of substrate (p-nitrophenol palmitate, 2.5–10 μg mL^{-1}). The kinetic parameters k_m and v_{max} were determined from Lineweaver Burk plot. To determine the type of enzyme inhibition, esterification reaction was performed in the mixture containing various concentration of chlorpyrifos in the range of 0.2–1.0 mgL^{-1}.

2.5. Effect of paper dimension on precision

To comprehend the influence of background noise, functional PBD was prepared in three dimensions. Category A was 1.5 × 12.5 cm, w x l. Category B and C were 1.5 × 10.0 cm and 1.5 × 7.5 cm, respectively. The concentration of enzyme and substrate were kept constant in all the three category. The distance between the enzyme zone and reaction zone varied. Performance of these three functional paper sensors were evaluated based on the mean Cb values in ROI and background zone. The category which showed less or nil background noise was chosen for further study.

2.6. Effect of pH on the performance of the paper-based device

To determine the influence of sample solution's pH on quantitative assessment of enzyme-substrate reaction, the performance of functional paper PBD was evaluated at different pH in the range of 5.0–9.0. The functional paper biosensors containing 5 μL of p-NPP (5 mg mL^{-1}) and 10 μL of lipase (1.0 mg mL^{-1}) were placed separately in buffer having adjusted pH. The mean Cb values in ROI and background zone were measured. Enzyme activity was determined and discussed.

2.7. Storage stability of paper-based device

Batch of PBD with the dimension of 7.5 × 1.5 cm was prepared and loaded with 5 μL of p-NPP (5 mg mL^{-1}) and 10 μL of lipase (1 mg mL^{-1}). The functional paper PBD were stored at 4 °C for the period of 30 days. Storage stability of the sensor was explored on every 3 days under optimal experimental conditions. The mean of the relative activity to the initial activity was plotted as a function of time. Similarly, the influence of PBD exposure temperature and time before the start of the experiment were investigated. The functional PBD were kept at different temperature (24 °C, 37 °C, 40 °C, 45 °C) for 60 min. Enzyme activity was determined for every 15 min and the relative activity to the 0 min activity at 37 °C was calculated. Enzyme activity retention in PBDwas tested at different temperature, considering the work place could be with or with-out air conditioner. Further, it was considered that the PBD could be used in the field where the temperature is higher. In India, the average temperature during the summer, the temperature ranges from 40 to 45 °C. Hence, the activity retention in PBD was tested at 24 °C, 37 °C, 40 °C and 45 °C.

2.8. Effect of ions and detergents on the performance of paper biosensor

The effect of various ions and detergents present in the water samples on the performance of PBD was studied. Water samples with the following ions Ca^{2+}, Cu^{2+}, Fe^{2+}, Pb^{2+}, Mg^{2+}, Zn^{2+} and Cd^{2+} and were prepared at the concentrations (mgL^{-1}) of 370, 0.25, 5.0, 0.05, 150, 25 and 0.015 respectively. Similarly, the effect of anionic, cationic and non-ionic detergents such as sodium dodecyl sulfate, cetrimonium bromide and triton X-100, respectively were studied at 0.01% concentration. The functionalized PBD was placed separately in water containing ions and detergents, and was allowed to react with the substrate. The relative activity was calculated from the activity measured in distilled water.

2.9. Method validation

A total of 10 different commonly consumed commodity fruits and vegetables were collected from local market for the analysis of chlorpyrifos determination using functionalized PBD. The samples included four fruits (grape, orange, apple, pomegranate) and six vegetables (tomato, cabbage, cauliflower, brinjal, green chilli and coriander leaves). One kilograms of each fruits and vegetables were collected through random sampling from different merchants. All the samples in a sterile polythene bag was transported carefully to the laboratory without any contamination and deterioration. Each representative fruits and vegetables were washed thoroughly in sterile water at 1:1 w/v ratio. Wash water was tested for the presence of chlorpyrifos using functionalized PBD as well as in micro titre plate assay method. The intention of these two methods was to compare the results obtained. The error percentage in determining pesticide concentration by these two methods was calculated using the following equation.

$$Error\,(\%) = \frac{([Pesticide]_{M1} - [Pesticide]_{M2})}{[Pesticide]_{M1}} \times 100$$

where, M1 and M2 are microtiter plate assay and image processing methods, respectively.

The linearity of enzyme inhibition with chlorpyrifos concentration in the range of 0.1–1.0 mgL^{-1} was investigated. The method precision was determined by triplicate analysis in distilled water using functionalized PBD under optimal conditions. The quantitative analysis of chlorpyrifos was performed by image processing analysis based on the corrected mean Cb value. According to Shrivastava [24], the limit of detection (LOD) and Limit of quantification (LOQ) were estimated at signal to noise ratio of 3 (S/N = 3) and 10 (S/N = 10), respectively.

2.10. Statistical analysis

All the experiments in this study was performed in triplicate and the results were calculated as mean ± SD. Statistical analysis was done using ANOVA in Origin Pro 2018 software and the probability value 0.05 or less was considered as significant.

3. Result and discussion

3.1. Selection of colour space and coordinate

The selection of colour space for quantitative description of targeted compound in image processing is generally a challenging one. Hence, the original image is converted into various colour space models to

determine the profile of each colour coordinates. The present work aims at identifying the best colour space model and colour coordinate to determine the p-nitrophenol concentration based on the high R^2 value in linear regression plot. Four important colour spaces models such as Grey, RGB, HSV and YCbCr are selected for this study. These colour spaces are geometrical representation of colours in a space by means of numerical values mainly by three components. Most common colour space is RGB and is normally the default colour space for representing digital images in camera, mobile phone, computers, graphics cards and LCDs. It consists of three primary colours components, red, green and blue. HSV colour space is a nonlinear transform of the RGB colour space, which is chosen for its ability to distinguish the hue (amount of grey) and brightness or intensity. YCbCr colour space is commonly used in television transmission. Since YCbCr colour space makes it easy to get rid of some redundant colour information which is widely used in digital video domain. In YCbCr, luminance information is stored as a single component (Y), and chrominance information is stored as two colour-difference components (Cb and Cr). The separation of luminance from chrominance is more effective in HSV and YCbCr models. In general, CMYK colour space model is widely be used for lighter colours like yellow. But, the present study considered that the algorithm should be useful to detect any other colour bar codes which will be printed on the PBD for tracking purposes.

In the present study, a calibration curve for the determination of p-nitrophenol concentration on paper support is constructed for each coordinate of RGB, HSV and YCbCr colour space using image processing algorithm. Table 1 shows the statistics obtained in each colour space in image processing method. 10 µL of p-nitrophenol solution (0.25–25 µg mL^{-1}) was applied on paper support (1 × 1 cm) at ROI and allowed to dry for 15 min. Then, the image of paper strip was captured and the change in the individual colour coordinate with respect to p-nitrophenol concentrations was measured. As shown in Fig. S5a, mean grey intensity value linearly increased with p-nitrophenol concentration up to 12.5 µg mL^{-1} followed by a drastic dip at 15 µg mL^{-1}. Further increase in the p-nitrophenol concentration resumed the mean intensity value increases. Similar trend was observed in all the colour coordinate of RGB colour space model (Fig. S5b). In HSV colour space model, the value of H (hue) does not show any significant difference with p-nitrophenol concentrations. A decreasing trend was observed for the coordinate S (saturation) while increasing p-nitrophenol concentrations. Whereas, the coordinate V (value) followed a pattern as seen in RGB colour space model (Fig. S5c). In YCbCr colour space model, no significant change in the value of Cr was observed. The changes in the values of mean of YCbCr and Y coordinate were mentioned in RGB colour space model. The Cb coordinate of YCbCr showed a significant linearity, with the concentration of p-nitrophenol (Fig. S5d). To understand the batch variation, p-nitrophenol calibration curve was constructed from images taken in two set of experiments (2.5–12.5 µg mL^{-1} concentrations with triplicate in one set and 15–25 µg mL^{-1} concentrations with triplicate in another set). The light illumination in both the set images were different. The effect of illumination was seen on the intensity profile of certain colour coordinates and caused shifting exactly at 15 µg mL^{-1} concentration. Higher influence of illumination was observed in colour coordinates such as mGray, mR, mG, mB, mV, mY, mRGB and mYCbCr. The influence of illumination in intensity profile of mS was very low. The HSV colour space is a nonlinear transform of the RGB colour space, which perfectly separates the luminance component from the chrominance information. However, the coefficient of determination for mS was found to be 0.816. No illumination effect was observed in the intensity profile of mCb and mCr. In general, the YCbCr colour space divide the input image into one luminance (Y) channel and two chromo (Cb and Cr) channels. The Cb and Cr coordinates showed the difference of blue and red component, respectively. The Cb coordinate showed a significant linearity, whereas Cr coordinate remained constant for all the p-nitrophenol concentrations tested. Hence, mCb was considered as most reliable indicator for measuring the p-nitrophenol concentration. Further, the result also showed that the mCb value for the image remain constant for more than 60 min of exposure time. Hence, YCbCr colour space model and Cb coordinate were considered as most reliable coordinate for measuring the p-nitrophenol concentration through image processing method. In addition to the effect of illumination, the auto-adjustment in smartphone camera has become a limitation. Most of the smart phone cameras have more green pixel to adequately record the information in green wavelength. Therefore, normalization functions such as fspecial and bsxfun were used in MATLAB algorithm to control the inhomogeneous intensity distribution in all the captured images. Fig. 2 depicts the comparative calibration curve for p-nitrophenol generated by microtiter plate method ($A410_{nm}$) and image processing method (mCb value). The results obtained from both the methods were comparable. Inorder to understand the linearity deviations in the calibration plot, studentized residual plot and relative error plot were constructed according to Jurado [25] (Fig. S6). The trend of residual points for Cb intensity values and A_{410nm} were closer to each other. In relative error plot, the deviations from the linearity for Cb values were comparatively low and closer to zero. According to Peter [26], luma guided anisotropic provides a significant high quality colour data. The report of Shu [27] et al. stated that the YCbCr colour space demonstrated more accurate results than CMYK colour model in analyzing the

Table 1
Statistics for the regression plot made between p-nitrophenol concentration and intensity of various colour space models. Results are representative of triplicates.

Parameter	Linear equation	R^2
mR	Y = 0.1186 X + 0.0026	−0.029
mG	Y = 0.1213 X + 0.0022	−0.062
mB	Y = 0.1493 X + 0.0073	0.279
mRGB	Y = 0.1297 X + 0.0040	0.060
mGray	Y = 0.0039 X + 0.108	0.051
mH	Y = 0.0000 X - 0.0013	−0.124
mS	Y = −0.0085 X - 0.0433	0.816
mV	Y = 0.0033 X + 0.0593	0.022
mHSV	Y = − 0.0017 X + 0.0048	0.404
mY	Y = 0.6206 X + 17.4666	0.072
mCb	Y = 0.6177 X + 0.0666	0.988
mCr	Y = − 0.0582 X - 1.2	0.120
mYCbCr	Y = 0.3934 X + 5.4444	0.359

Y is mean intensity value; X is concentration of p-nitrophenol.

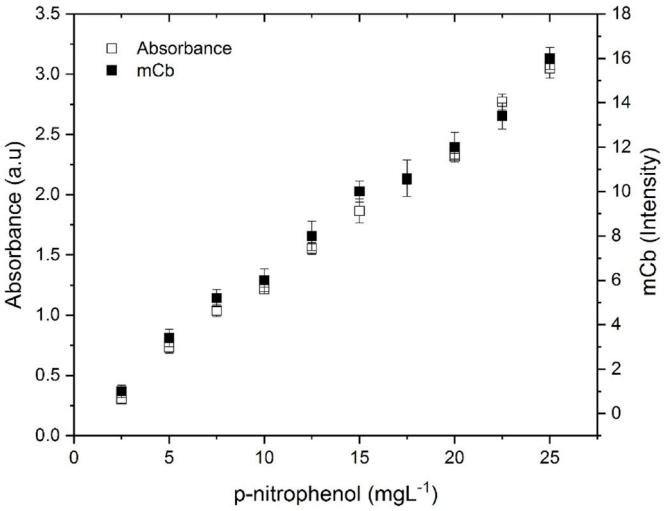

Fig. 2. Calibration curve of p-nitrophenol quantification as function of mCb intensity (image processing method) and absorbance at 410 nm (microtiter plate assay method). Data are means of triplicates and the error bars are ± SD.

Table 2
Kinetic parameters of free and paper immobilized *Rhizopus niveus* lipase with and without inhibition. Data are reported as mean ± SD for n = 3.

[I], mgL^{-1}	Free enzyme		Immobilized Enzyme	
	K_m	V_{max}	K_m	V_{max}
Un Inhibited	4.72 ± 0.30	165.9 ± 6.87	8.97 ± 1.25	151.82 ± 8.48
2.0	6.15 ± 0.32	164.9 ± 3.10	9.13 ± 0.90	144.26 ± 2.43
4.0	8.37 ± 0.54	169.6 ± 5.06	16.24 ± 2.17	160.86 ± 10.05
6.0	10.96 ± 0.71	169.6 ± 5.1	32.79 ± 9.69	151.48 ± 13.19
8.0	31.36 ± 0.79	201.5 ± 6.26	55.33 ± 4.0	153.68 ± 12.05

colour stained images of human oesophageal cancer, colon cancer and liver cirrhosis. In another clinical diagnosis studies, Cr coordinate of the YCbCr showed 93.875 classification accuracy in distinguishing cancer and non-cancerous cells [28]. Miyazaki [29] obtained a linear regression between the mass of powdered formulated medicine and Cb coordinate value with R^2 of 0.98.

3.2. Enzyme and inhibition kinetics

Preliminary experiments were designed to understand the kinetic parameters of free and immobilized *Rhizopus niveus* lipase according to Michalis Menten single substrate reaction kinetic equation. The free enzyme activity of *Rhizopus niveus* lipase was estimated spectrophotometrically at various substrate concentration ranging from 2.5 to 10 μg mL^{-1}. From Lineweaver-Burk plot, the kinetic parameters, K_m and V_{max} were determined to be 4.75 μg mL^{-1} and 166.7 Umg^{-1}, respectively (Fig. S7). Whereas, the enzyme activity of the immobilized lipase on paper was determined through image processing technique and the K_m of 9.75 μg mL^{-1} and V_{max} of 144.9 Umg^{-1} were determined from respective Lineweaver-Burk plot (Fig. S8). The reaction rate of the paper immobilized lipase was comparatively lower than that of free enzyme. Conversely, the K_m value of immobilized enzyme was increased twofold than free enzyme (Table 2). It is worthy to note that the reduced enzyme activity after immobilization on Whatman No.1 paper could be due to irregular orientation of the active sites of bound enzyme. Further, an ionic interaction between the enzyme and matrix would be established. Hence, the immobilized enzyme activity decreased [30].

Inorder to comprehend the type of enzyme inhibition, enzyme reaction was performed in the presence of chlorpyrifos at varying concentration in the range of 0.1–1.0 mgL^{-1}. The kinetic parameters K_m and V_{max} values were determined form double reciprocal Lineweaver-Burk plot for each reaction set up. Figs. S9 and S10 shows the inhibition plot for free and paper immobilized lipase, respectively. The determined K_m value for the reactions with pesticide is changed while V_{max} is unchanged. The K_m value for the reaction mixture containing 0.2, 0.4 and 0.6 mgL^{-1} of chlorpyrifos were 7.48, 11.43 and 15.27 μg mL^{-1}, respectively. In all the reaction setup including control (without pesticide), the V_{max} value was in the range between 144.9 and 151.5 Umg^{-1}. According to Palmer [31], it was inferred that chlorpyrifos competitively inhibit the paper bound *Rhizopus niveus* lipase. In this competitive inhibition, both p-nitrophenol palmitate and chlorpyrifos compete for the same active site on lipase leading to the decrease in the velocity of the reaction. Previously, an in-vitro acetylcholine esterase enzyme inhibition study conducted by Rao [32], stated that chlorpyrifos exhibits a concentration dependent on competitive inhibition. Whereas, Basica [33] reported that chlorpyrifos has allosteric activation-like effect on Glutathione S-transferases.

3.3. Effect of paper size

The conversion of colourless substrate (p-nitrophenol palmitate) into yellow coloured product (p-nitrophenol) is based on the available active enzyme at the reaction zone. The movement and distribution of enzyme molecules from enzyme zone to reaction zone depends on solubility, polarity and the distance between enzyme zone and reaction zone. Hence, we designed three set of paper sensors with different conformations, but concentration of substrate and enzyme were kept constant. Category A, paper size is 12.5 cm length and 1.5 cm width, in which the distance between enzyme zone and substrate zone was 8 cm. In category B sensor (10 cm × 1.5 cm), the distance was 5.5 cm. Similarly, 2.5 cm distance was provided in paper sensor with dimension of 7.5 cm × 1.5 cm (Category C). Three types of paper sensors were tested for its efficiency in buffer solution with and without chlorpyrifos and the images are provided in supplementary data (Fig. S12). Mean Cb values at reaction zone and background zone were determined through image analysis and signal to noise ratio (SNR) was calculated to choose the best paper dimension. According to Wang [34] the higher SNR indicates the best quality of image. The SNR above 20 and 32.04 dB indicates the image quality is an excellent and acceptable, respectively. In the present study, higher SNR was found to be 58 ± 2.6 in the paper size category C. The category A and B showed SNR values of 7 ± 0.43 and 14 ± 1.38, respectively (Table S1). It was lower than the acceptable range. Hence, the category C (7.5 × 1.5 cm) with the higher SNR values was chosen for lateral flow assay in further studies. Short distance (2.5 cm) between the enzyme and substrate zones in paper size category C might have facilitated the optimum binding of pesticide as a competitive inhibitor. Whereas in the paper size Category A and B, the distance between the enzyme zone and substrate zone is higher (8 and 5.5 cm, respectively). It takes longer time for an enzyme to reach the substrate zone. It might have caused the separation of enzyme and inhibitors.

3.4. Effect of sample solution pH on performance of paper-based device

The pH of reaction environment plays a vital role in enzyme substrate reaction due to the presence of ionizable group of amino acids in their structure. Hence in the present study, the pH of the sample solution is artificially varied in the range between 5.0 and 9.0, and the effect on PBD response is investigated. As shown in Fig. 3, *Rhizopus niveus* lipase exhibits a stable activity at wider pH range and the results agree with the report of Rabbani [35]. The relative activity at acidic pH was comparatively lower than that of alkaline pH. Relative activity of 88% was observed at pH 5.0. Whereas at pH of 9.0, it was 92%. Similarly, Andreescu [36] studied the pH effect on the performance of an amperometric biosensor and obtained a good response between the pH 5 and 9. Zang [37] reported that an enzyme doped biosensor is very active only in the pH range between 6.5 and 7.0 in detection of paraoxan.

3.5. Storage stability of the functional paper-based device

The storage stability and activity retention of lipase doped PBD was evaluated. The functional PBD was stored at 4 °C after the fabrication and its response at optimal experimental conditions was recorded on every three days for the period of 30 days. The profile of mean Cb values shows that the enzyme doped PBD retained the activity of 97% till 15th day, while decrement of the response was recorded to 87.4%

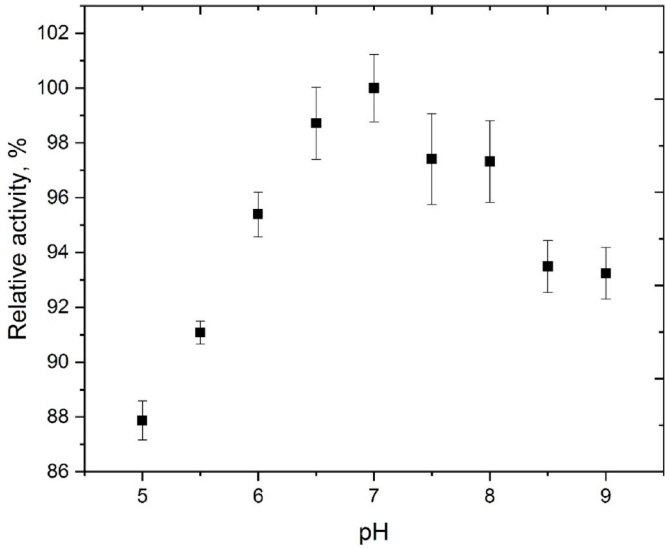

Fig. 3. Effect of sample's pH on the performance of PBD. Data are means of triplicates and the error bars are ± SD.

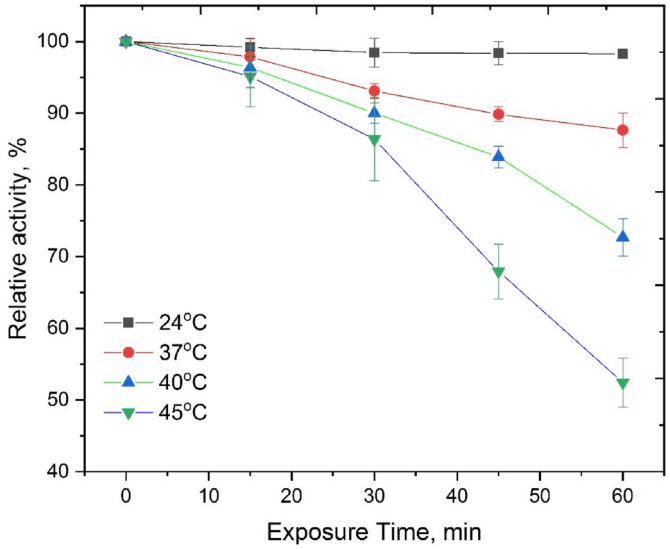

Fig. 5. Activity retention in functionalized PBD exposed at different temperature. Data are means of triplicates and the error bars are ± SD.

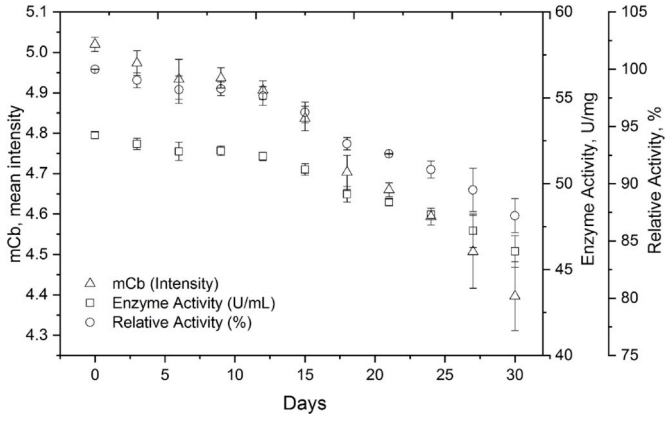

Fig. 4. Storage stability of functionalized paper-based device at 4 °C. Data are means of triplicates and the error bars are ± SD.

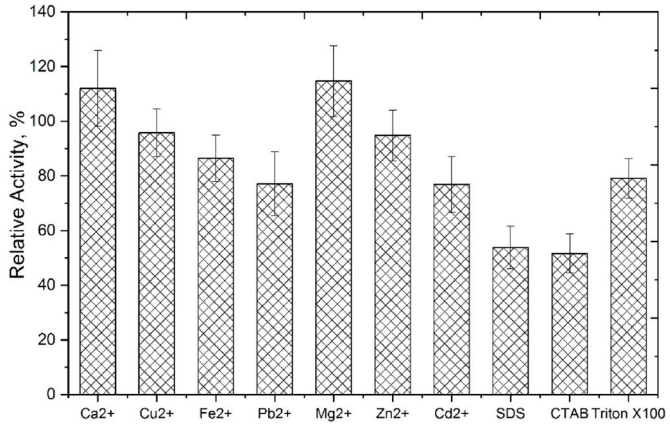

Fig. 6. The effect of various ions and detergents on the performance of *Rhizopus niveus* lipase. The ion concentrations are Ca^{2+} (370 mgL^{-1}), Mg^{2+} (150 mgL^{-1}), Cu^{2+} (0.25 mgL^{-1}), Zn^{2+} (25 mgL^{-1}), Fe^{2+} (5.0 mgL^{-1}), Pb^{2+} (0.05 mgL^{-1}) and Cd^{2+} (0.015 mgL^{-1}). All the detergents are tested at 0.01% concentration. Data are means of triplicates and the error bars are ± SD.

on 30th day (Fig. 4). A considerable good activity retention up to four weeks indicated the good stability of doped lipase enzyme on functionalized PBD. Similar study was conducted by Lei [38] using organophosphorus hydrolase for the detection of organophosphate pesticides and reported that the storage life of developed amperometric biosensor is about 2 days at 4 °C.

Inorder to evaluate the stability of functionalized PBD better at different operational temperatures, the PBD was exposed at 24 °C, 37 °C, 40 °C and 45 °C separately, for 60 min. Fig. 5 shows that the activity retention at 24 °C is stable and further increase in the temperature resulted a decreasing trend in activity retention. Only half of its initial activity was measured at 45 °C after 60 min. The PBD exposed to 37 °C and 40 °C for 60 min showed 84.9 and 75.2% of relative activity.

3.6. Effect of metal ions and detergents on the performance of functional paper-based device

Besides pesticide, there are compounds like drugs, metal ions and natural phyto compounds show affinity toward lipases and may potentially inhibit the lipase activity. A detailed literature survey inferred that the inhibitors have different affinity profile towards different lipases. *Pseudomonas* lipase is inhibited by Fe (III+), sodium dodecyl sulfate, *n*-dodecyltrimethylammonium bromide, sorbitan monooleate. Lipase from *Yarrowia lipolytica* is inhibited by wide range of metal ions (Hg^{2+}, Ni^{2+}, Cu^{2+}, Zn^{2+}). Range of alcohols shows inhibitory role against *Geobacillus* lipase [39]. Hence in the present study, various ions and detergents are tested for its effect on the performance of PBD. The concentrations up to five times higher than the Bureau of Indian Standards (BIS) 2012; IS: 10500 [40] for drinking water is tested on its effect against *Rhizopus niveus* lipase. Fig. 6 shows that the presence of Ca^{2+} (370 mgL^{-1}) and Mg^{2+} (150 mgL^{-1}) in water samples slightly enhanced lipase activity. Cu^{2+} and Zn^{2+} at 0.25 and 25 mgL^{-1} respectively maintained the lipase activity. Conversely, the ions such as Fe^{2+} (5.0 mgL^{-1}), Pb^{2+} (0.05 mgL^{-1}) and Cd^{2+} (0.015 mgL^{-1}) showed a negative effect on the lipase activity and reduced around 10–20% of its original activity. However, the inhibition by certain ions is recorded in this study, the chlorpyrifos exhibited higher amount of inhibition. Further the enzyme kinetic studies revealed that the affinity of chlorpyrifos was higher than that of other intermediates.

The detergents (SDS, CTAB and triton X-100) at 0.01% significantly reduced the lipase activity which was closer to the inhibition by chlorpyrifos at 0.2 mgL^{-1}. Hence, the presence of detergents may limit the accuracy of PBD in detection of chlorpyrifos.

Table 3
Comparison of the efficiency of the image processing method and microtiter plate method for the determination of chlorpyrifos in artificial pesticide water.

Chlorpyrifos in APW (mgL^{-1})	n	MTPM			IMGPM		
		Determined Chlorpyrifos (mgL^{-1})	SD	Recovery (%)	Determined Chlorpyrifos (mgL^{-1})	SD	Recovery (%)
0.2	3	0.219	0.007	94	0.220	0.013	87
0.5	3	0.534	0.014	108	0.542	0.012	106
1.0	3	1.091	0.004	101	1.134	0.012	109

APW – Artificial pesticide water; MTPM – Microtiter plate method; IMGPM – Image processing method; SD – Standard deviation; n - number of samples.

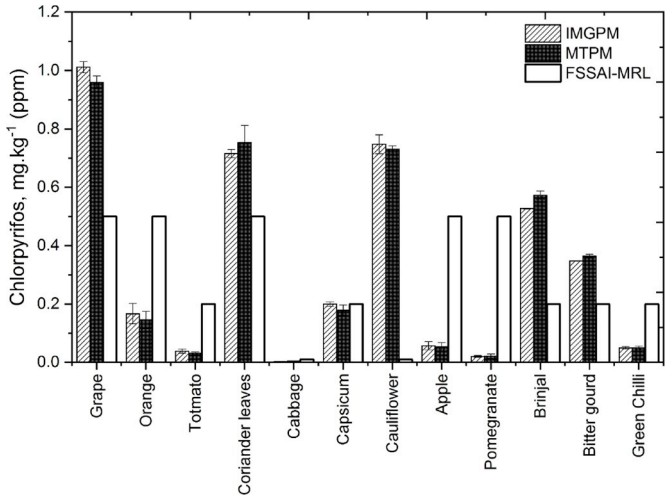

Fig. 7. Comparison of the results obtained for chlorpyrifos determination in wash water of selected fruits and vegetables using image processing method and microtiter plate assay method with FSSAI- MRL standard. Data are means of triplicates and the error bars are ± SD.

3.7. Method validation

The ability to detect small amount of pesticide present in a solution using functionalized PBD was determined through the limit of detection and limit of quantification. A calibration curve for chlorpyrifos concentration (0.1–1.0 mgL^{-1}) against enzyme inhibition (%) was constructed and the coefficient of determination was found to be 0.998 (supplementary data). Based on the standard deviation of three repeated values, the limit of detection (LOD) and limit of quantification (LOQ) were calculated as 0.06 mgL^{-1} and 0.198 mgL^{-1}. As shown in Table 3, the recovery percentage of chlorpyrifos in artificial pesticide water determined using the image processing method is closer to values determined in standard microtiter plate method.

To comprehend the efficiency of functionalized PBD in real time applications, wash water was prepared for selected fruits and vegetables as mentioned in the methodology section and used as sample to determine the pesticide concentration. Further, the developed image processing method of detection was compared with standard colourimetric assay (microtiter plate assay method).

Among all the fruits and vegetables wash solutions tested, cauliflower, grapes, coriander leaves, brinjal and bitter guard were found having higher maximum residue level (MRL) (Fig. 7). The chlorpyrifos residues in wash water of apple, pomegranate, orange, tomato, green chilli and cabbage were lower than that of FSSAI-MRL. In capsicum, the chlorpyrifos residue was closer to the MRL value. Angioni [41] reported MRL of chlorpyrifos in orange, grapes and tomatoes as 0.3, 0.5, and 0.5 mg kg^{-1}, respectively. The low error percentage between IMGPM and MTPM of the current study indicates that image processing can be applied to the detection of chlorpyrifos in any fruit and vegetable wash water.

4. Conclusion

The present study describes the development of functionalized paper-based device for chlorpyrifos detection in water samples. The quantitative analysis relies on the principle of enzyme inhibition and image processing concepts. Best of our knowledge, single colour coordinate Cb of YCbCr colour space was demonstrated for the determination of chlorpyrifos for the first time. The LOD of 0.06 mgL^{-1} demonstrates the developed paper PBD which is most suitable for determining the pesticide concentration in fruits and vegetable wash waters. Further, it exhibits the same bioanalytical performance as the standard microtiter plate method for the detection of chlorpyrifos. Image processing is the basis of the newly developed assay in the current study, and it offers several advantages towards the development of android mobile application and PoC based analysis. The future studies will be on pretreatment of paper support and microfluidic enzyme reaction systems to improve the limit of detection.

Acknowledgement

Authors express gratitude to Tamilnadu State Council for Science and Technology, Chennai and Department of Biotechnology, Kamaraj College of Engineering and Technology, K. Vellakulam, Madurai, Tamilnadu for providing support to complete the project. Authors express gratitude to S. Athithya, S. Vidya Sankari, P. Saranya, R.K.Akashkumar, G.R.Murari Viyas, K. Naresh and S. Vaitheeswaran for the support during preliminary experimental studies. Authors also thank Dr.B.Kayal vizhi for her help during proof reading.

Appendix A. Supplementary data

Supplementary data to this article can be found online at https://doi.org/10.1016/j.talanta.2019.120408.

References

[1] S. Kumar, G. Kaushik, J. Villarreal-Chiu, Scenario of organophosphate pollution and toxicity in India: a review, Environ. Sci. Pollut. Res. 23 (2016) 9480–9491 https://doi.org/10.1007/s11356-016-6294-0.
[2] K. Christensen, B. Harper, B. Luukinen, K. Buhl, D. Stone, Chlorpyrifos technical fact sheet, national pesticide information center, Oregon State University Extension Services, 2009, http://www.npic.orst.edu/factsheets/chlorpgen.html , Accessed date: 11 August 2019.
[3] A.L. Rathod, R.K. Garg, Chlorpyrifos poisoning and its implications in human fatal cases: a forensic perspective with reference to Indian scenario, J Forensic Leg Med 47 (2017) 29–34 https://doi.org/10.1016/j.jflm.2017.02.003.
[4] D.M. Ferre, A.A.M. Quero, A.F. Hernandez, V. Hynes, M.J. Tornello, C. Luders, N.B.M. Gorla, Environ. Monit. Assess. 190 (5) (2018) 292 https://doi.org/10.1007/s10661-018-6647-x.
[5] Jesus Lozano, Apetrei Constantin, Mahdi Ghasemi-Varnamkhasti, Daniel Matatagui, José Pedro Santos, Sensors and systems for environmental monitoring and control, J. Sensors 2 (2017), https://doi.org/10.1155/2017/6879748.
[6] X. Luo, J. Yang, A survey on pollution monitoring using sensor networks in environment protection, J. Sensors 11 (2019), https://doi.org/10.1155/2019/6271206.
[7] C.I.L. Justino, A.C. Duarte, T.A.P. Rocha-Santos, Recent progress in biosensors for environmental monitoring: a review, Sensors 17 (12) (2017), https://doi.org/10.3390/s17122918.
[8] M. Pohanka, D. Jun, K. Kuca, Amperometric biosensors for real time assays of organophosphates, Sensors 8 (9) (2008) 5303–5312 https://doi.org/10.3390/

s8095303.
[9] A. Singh, A.W. Flounders, J. Volponi, C.S. Ashley, K. Wally, J.S. Schoeniger, Development of sensors for direct detection of organophosphates. Part I: immobilization, characterization and stabilization of acetylcholinesterase and organophosphate hydrolase on silica supports, Biosens. Bioelectron. 14 (8–9) (1999) 703–713 https://doi.org/10.1016/S0956-5663(99)00044-5.
[10] S. Stepankova, K. Vorcakova, Cholinesterase-based biosensors, J. Enzym. Inhib. Med. Chem. 31 (sup3) (2016) 180–193 https://doi.org/10.1080/14756366.2016.1204609.
[11] H.Y. No, Y.A. Kim, Y.T. Lee, H.S. Lee, Cholinesterase-based dipstick assay for the detection of organophosphate and carbamate pesticides, Anal. Chim. Acta 594 (1) (2007) 37–43 https://doi.org/10.1016/j.aca.2007.05.008.
[12] Hyeok Jung Kim, Yeji Kim, Su Jung Park, Chanho Kwon, Hyeran Noh, Development of colourimetric paper sensor for pesticide detection using competitive-inhibiting reaction, BioChip J. 12 (4) (2018) 326–331 https://doi.org/10.1007/s13206-018-2404-z.
[13] Panpan Gai, Shuxia Zhang, Yu Wen, Haiyin Li, Feng Li, Light-driven self-powered biosensor for ultrasensitive organophosphate pesticide detection *via* integration of the conjugated polymer-sensitized CdS and enzyme inhibition strategy, J. Mater. Chem. B. 6 (42) (2018) 6842–6847 https://doi.org/10.1039/C8TB02286K.
[14] J. Kumar, S.K. Jha, S.F. D'Souza, Optical microbial biosensor for detection of methyl parathion pesticide using Flavobacterium sp. whole cells adsorbed on glass fiber filters as disposable biocomponent, Biosens. Bioelectron. 21 (11) (2006) 2100–2105 https://doi.org/10.1016/j.bios.2005.10.012.
[15] Y.A. Cho, G.S. Cha, Y.T. Lee, H.S. Lee, A dipstick-type electrochemical immunosensor for the detection of the organophosphorus insecticide fenthion, 6, Food Sci. Biotechnol. 14 (2005), pp. 743–746 https://www.earticle.net/Article/A78900.
[16] D.D. Liana, B. Raguse, J.J. Gooding, E. Chow, Recent advances in paper-based sensors, Sensors 12 (9) (2012) 11505–11526 https://doi.org/10.3390/s120911505.
[17] A.W. Martinez, S.T. Phillips, M.J. Butte, G.M. Whitesides, Patterned paper as a platform for inexpensive, low-volume, portable bioassays, Angew Chem. Int. Ed. Engl. 46 (8) (2007) 1318–1320 https://doi.org/10.1002/anie.200603817.
[18] W. Wang, W.Y. Wu, W. Wang, J.J. Zhu, Tree-shaped paper strip for semi-quantitative colourimetric detection of protein with self-calibration, J. Chromatogr. A 11 (24) (2010) 3896–3899 https://doi.org/10.1016/j.chroma.2010.04.017.
[19] W. Dungchai, O. Chailapakul, C.S. Henry, Use of multiple colourimetric indicators for paper-based microfluidic devices, Anal. Chim. Acta 674 (2) (2010) 227–233 https://doi.org/10.1016/j.aca.2010.06.019.
[20] K. Thajee, P. Paengnakorn, W. Wongwilai, K. Grudpan, Application of a webcam camera as a cost-effective sensor with image processing for dual electrochemical - colourimetric detection system, Talanta 185 (2018) 160–165 https://doi.org/10.1016/j.talanta.2018.03.055.
[21] N. Jiang, W. Song, H. Wang, G. Guo, Y. Liu, Differentiation between organic and non-organic apples using diffraction grating and image processing-A cost-effective approach, Sensors 18 (6) (2018), https://doi.org/10.3390/s18061667.
[22] K. Sankar, A. Achary, Synthesis of feruloyl ester using Bacillus subtilis AKL 13 lipase immobilized on celite(R) 545, Food Technol. Biotechnol. 55 (4) (2017) 542–552 https://doi.org/10.17113/ftb.55.04.17.5331.
[23] E. Carrilho, A.W. Martinez, G.M. Whitesides, Understanding wax printing: a simple micropatterning process for paper-based microfluidics, Anal. Chem. 81 (16) (2009) 7091–7095 https://doi.org/10.1021/ac901071p.
[24] A. Shrivastava, V. Gupta, Methods for the determination of limit of detection and limit of quantitation of the analytical methods, Chronicles Young Sci. 2 (1) (2011) 21–25 https://doi.org/10.4103/2229-5186.79345.
[25] J.M. Jurado, A. Alcázar, R. Muniz-Valencia, S.G. Ceballos-Magana, F. Raposo, Some practical considerations for linearity assessment of calibration curves as function of concentration levels according to the fitness-for-purpose approach, Talanta 1 (172) (2017) 221–229 https://doi.org/10.1016/j.talanta.2017.05.049.
[26] P. Peter, L. Kaufhold, J. Weickert, Turning diffusion-based image colourization into efficient colour compression, IEEE Trans. Image Process. : a publ. IEEE Signal Process. Soc. 26 (2) (2017) 860–869 https://doi.org/10.1109/TIP.2016.2627800.
[27] J. Shu, G.E. Dolman, J. Duan, G. Qiu, M. Ilyas, Statistical colour models: an automated digital image analysis method for quantification of histological biomarkers, Biomed. Eng. Online 15 (2016) 46 https://doi.org/10.1186/s12938-016-0161-6.
[28] S. Jitaree, A. Phinyomark, P. Boonyaphiphat, P. Phukpattaranont, Cell type classifiers for breast cancer microscopic images based on fractal dimension texture analysis of image colour layers, Scanning 37 (2) (2015) 145–151 https://doi.org/10.1002/sca.21191.
[29] Y. Miyazaki, K. Miyawaki, T. Uchino, Y. Kagawa, Assessment of blending ratio of powdered medicine mixtures by image analysis, Chem. Pharm. Bull. 62 (4) (2014) 322–327 https://doi.org/10.1248/cpb.c13-00772.
[30] M.A. Abdel-Naby, A. Fouad, R.M. Reyad, Catalytic and thermodynamic properties of immobilized Bacillus amyloliquefaciens cyclodextrin glucosyltransferase on different carriers, J. Mol. Catal. B Enzym. 116 (2015) 140–147.
[31] T. Palmer, P.L.R. Bonner, Enzymes : Biochemistry, Biotechnology and Clinical Chemistry, Horwood Publishing, Chichester, 2007.
[32] J.V. Rao, P. Kavitha, In vitro effects of chlorpyrifos on the acetylcholinesterase activity of euryhaline fish, Oreochromis mossambicus, Zeitschrift fur Naturforschung. C, J. Biosci. 65 (3–4) (2010) 303–306 https://doi.org/10.1515/znc-2010-3-420.
[33] B. Basica, I. Mihaljevic, N. Marakovic, R. Kovacevic, T. Smital, Molecular characterization of zebrafish Gstr1, the only member of teleost-specific glutathione S-transferase class, Aquat. Toxicol. 208 (2019) 196–207 https://doi.org/10.1016/j.aquatox.2019.01.005.
[34] Y. Wang, C. Kuang, Z. Gu, X. Liu, Image subtraction method for improving lateral resolution and SNR in confocal microscopy, Opt. Laser. Technol. 48 (2013) 489–494 https://doi.org/10.1016/j.optlastec.2012.11.018.
[35] G. Rabbani, E. Ahmad, N. Zaidi, S. Fatima, R.H. Khan, pH-Induced molten globule state of Rhizopus niveus lipase is more resistant against thermal and chemical denaturation than its native state, Cell Biochem. Biophys. 62 (3) (2012) 487–499 https://doi.org/10.1007/s12013-011-9335-9.
[36] S. Andreescu, A. Avramescu, C. Bala, V. Magearu, J.L. Marty, Detection of organophosphorus insecticides with immobilized acetylcholinesterase - comparative study of two enzyme sensors, Anal. Bioanal. Chem. 374 (1) (2002) 39–45 https://doi.org/10.1007/s00216-002-1442-4.
[37] S. Zhang, H. Zhao, R. John, Development of a quantitative relationship between inhibition percentage and both incubation time and inhibitor concentration for inhibition biosensors–theoretical and practical considerations, Biosens. Bioelectron. 16 (9–12) (2001) 1119–1126 https://doi.org/10.1016/S0956-5663(01)00240-8.
[38] Y. Lei, P. Mulchandani, W. Chen, J. Wang, A. Mulchandani, Whole cell-enzyme hybrid amperometric biosensor for direct determination of organophosphorous nerve agents with p-nitrophenyl substituent, Biotechnol. Bioeng. 85 (7) (2004) 706–713 https://doi.org/10.1002/bit.20022.
[39] M. Pohanka, Biosensors and bioassays based on lipases, principles and applications, a review, Molecules 24 (3) (2019) 616–630 https://doi:10.3390/molecules24030616.
[40] A.K. Haritash, Shalini Gaur, Sakshi Garg, Assessment of water quality and suitability analysis of River Ganga in Rishikesh, India, Appl. Water Sci 6 (4) (2016) 383–392 https://doi:10.1007/s13201-014-0235-1.
[41] A. Angioni, F. Dedola, A. Garau, G. Sarais, P. Cabras, P. Caboni, Chlorpyrifos residues levels in fruits and vegetables after field treatment, J. Environ. Sci. Health B 46 (6) (2011) 544–549 https://doi.org/10.1080/03601234.2011.583880.